LOW-VELOCITY OBLIQUE IMPACT EXPERIMENTS IN A VACUUM. K. K. Hessen[1], R. R. Herrick[1], S. Yamamoto[2], O. S. Barnouin-Jha[3], S. Sugita[2], and T. Matsui[2], [1]Geophysical Institute, University of Alaska Fairbanks, Fairbanks, AK 99775-7320 (khessen@gi.alaska.edu); [2]Dept. of Complexity Science and Engineering, University of Tokyo, Japan; [3]The Johns Hopkins University Applied Physics Laboratory, Laurel, MD.

Introduction: Planetary impacts occur at nonvertical angles, so experimental studies of oblique impacts are useful for comparison with planetary craters. We conducted a set of experiments to expand upon previous studies, particularly those of Gault and Wedekind [1]. The raw data for [1] is no longer available, and we wish to explore details not observable in the published work. This includes finer angle increments than presented in [1] and videos of ejecta curtain development. Our experiments are at lower velocities than those for the images presented in [1] and can be used to consider differences between oblique primaries and secondaries.

Methodology: Experiments were conducted at the Impact Cratering Laboratory at the Department of Complexity Science, University of Tokyo Kashiwa. Polycarbonate projectiles (mass 0.49g, length 0.8cm, diameter 1.0cm) were launched from a single-stage light-gas gun into a chamber capable of near-vacuum pressure conditions. The chamber has ports for mounting the gun at 15° increments from 90° to 15°. Impact angles ranging from 90° to 0.5° were achieved by tilting the target container up to 15° from horizontal.

The target was prepared by filling a bowl inside the vacuum chamber with brown basaltic sand (grain size less than 500 microns, density 1.44g/cc) and then dusting the sand surface with white flour to make the ejecta easily distinguishable from the target surface. Cohesion of the target material was similar to the shots of [1] into quartz sand, but lower than their shots into pumice (and consequently less likely to preserve steep interior slopes in the crater). The air was pumped out of the chamber until the pressure inside was below 100 Pa, after which the polycarbonate projectile was fired from the gun. Projectile velocities ranged from 144 m/s to 260 m/s ([1] explored this velocity range but only showed images from shots > 1 km/s). Each shot was imaged with a digital video recorder at 200 frames per second and digital images were acquired of the resulting crater. Crater diameter and depth were also measured for most craters either by taking a profile of the crater or measuring it directly with a ruler. Thirty-six successful shots were taken spanning the range of possible impact angles. Unlike [1] the impactor did not disrupt but instead usually ricocheted out of the target.

Results: *Crater Size.* Crater rim diameters decrease from just over 100 mm with a vertical impactor to ~40 mm at the lowest impact angles. Figure 1 shows how maximum crater diameter changes with impact angle. Variations may be due to the range of velocities in the experiments. A line of $D_{90°} \sin^{1/3}\Theta$ is shown in figure 1 to illustrate that diameter vs. impact angle approximately follows the same relationship as volume vs. Θ in [1] (those plots show displaced mass vs. Θ following a sinΘ trend).

Crater Shape. Craters remain circular down to impact angles of 15° from horizontal. Below 15°, craters become increasingly more elliptical as impact angle decreases. Figure 2 shows the dependence of crater shape on impact angle using crater elongation, defined here as the ratio of the maximum crater diameter to the minimum crater diameter.

Ejecta Distribution. Figures 3-6 illustrate the change in ejecta distribution as impact angle becomes increasingly horizontal. The ejecta begins to be asymmetric at impact angles of approximately 60° from horizontal (figure 4), and a clear uprange forbidden zone develops around 20°. As impact angle decreases below 20°, the uprange forbidden zone continues to increase in size, and less ejecta is located in the downrange direction. In contrast to the results of [1], there is always some ejecta present in the downrange direction, even at the lowest impact angles. This suggests that formation of the downrange forbidden zone in hypervelocity low-angle impacts may be tied to creation of a downrange traveling vapor cloud. Overall the morphological transitions occur at impact angles closer to vertical than observed on the moon [2] or the higher velocity experiments in [1].

References: [1] Gault, D. E. and Wedekind J. A. (1978) *Proc. LPSC 9th*, 3843-3875. [2] Herrick, R. R. and Forsberg-Taylor, N. K. (2003) *Met. and Planetary Science* 38:1551-1578.

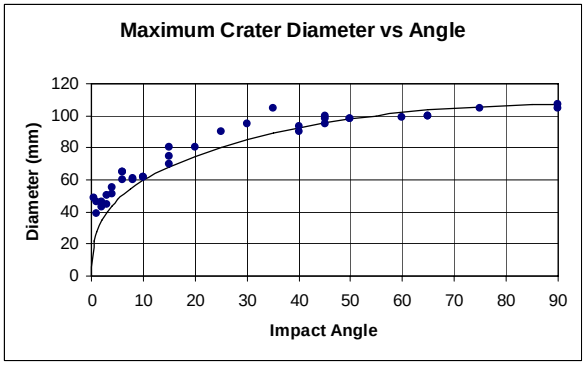

Figure 1. Maximum crater rim diameter for experimental impact craters created at different impact angles. Angles are measured from impact surface (90° is vertical). The solid curve is $D_{90°} \sin^{1/3}\Theta$.

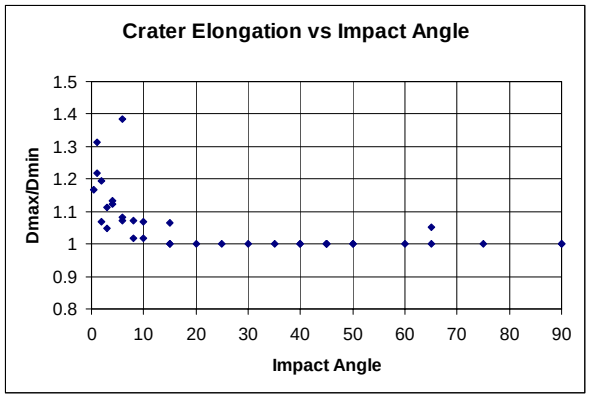

Figure 2. Dependence of crater elongation on impact angle. Crater elongation is D_{max} / D_{min}.

Figure 3. Vertical Impact **(**90°). Crater is 107 mm across. Ejecta is symmetric about the crater.

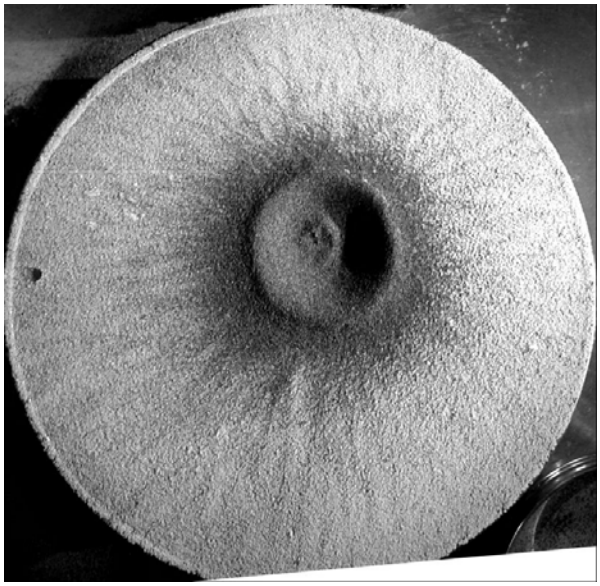

Figure 4 (bottom, previous column). 60° Impact. Crater is 99 mm across. Ejecta is beginning to be offset in the downrange direction. Projectile trajectory is from top to bottom.

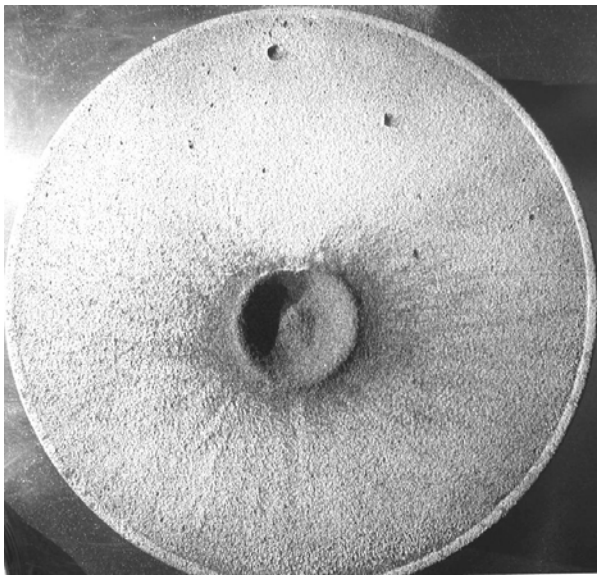

Figure 5. 20° Impact. Crater is 80 mm across. An uprange forbidden zone is beginning to form. Projectile trajectory is from top to bottom.

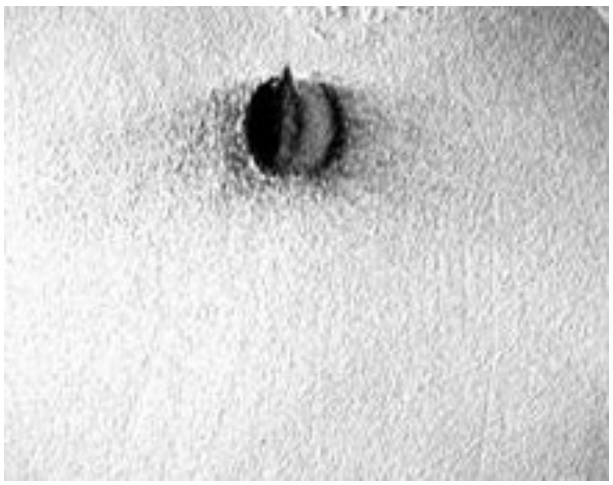

Figure 6. 0.5° Impact. Crater is 49 mm x 42 mm. Ejecta is concentrated in the crossrange direction, with some ejecta still present in the downrange direction. Projectile trajectory is from top to bottom.